

Important IP Data Responses Not Reproduced in Inversion Software - A Synthetic Study (1)

Preamble:

This study began as an interpretation project for a client and is based upon two actual datasets over the same survey area. We were asked to confirm the results that had been presented to the client which had been produced by a popular commercial IP inversion product. This request came as our forward modeling software was recommended to them in being able to simulate accurately many aspects of the responses contained in electric field surveys such as dipole-dipole, pole-dipole and gradient resistivity and induced polarization surveys. We would like to remind the reader that induced polarization surveys are an electric field problem with currents injected into the ground with these currents flowing throughout the subsurface and changing as they interact with the resistivity distribution in the ground. IP anomalies are not isolated anomalies without interactions with the background materials and other anomalies as occurs in gravity problems. The IP responses cannot be assumed to be due to the charges induced on the surface of anomalies simply by the injected currents.

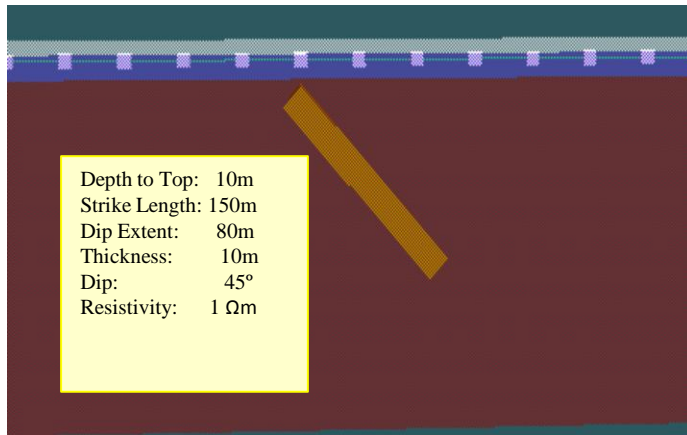
As we began to discover models which reproduced the data for both a gradient and a dipole-dipole survey, we realized that the incorrect interpretation by the inversion software was another instance of a forward algorithm not being able to reproduce current interactions between different structures in the resistivity distribution. In this case, the inversion software had not been able to resolve the effect of responses of the cover material upon the responses of both conductors and resistors below this cover. We had encountered this type of problem many times with several inversion products in regard to data from a number of clients dating back to the late 1990's. These inversion products invariably reproduced solutions which were more akin to potential field solutions .

Over a period of almost forty years, the author has studied, in detail, the capabilities of numerous algorithms developed for electric field problems in geophysics. What was discovered was that standard approaches to solving the electric field differential equations by finite difference, finite element and integral equation methods did not reproduce correctly current flow between different portions of the model's resistivity distribution. More simply put, the codes were not able to reproduce interactions between different portions of a resistivity model. These results led to studies into the source of this issue with the algorithms and methods to overcome these limitations.

This issue is not in the mathematical formulation of the algorithm but is rather a well known numerical issue known in many fields of physics and engineering. All inversions require a forward solution to the models generated by each iteration. All standard approaches to numerically solving differential equations suffer from this issue of weak interactions between bodies. The reason is simply because these techniques form a matrix then solve the matrix but the matrix solvers are the source of the numerical limitations. In the electric field problems, the elements on the diagonal of this matrix are the self scattering terms or the responses of the inversion grid cells in isolation. The diagonal terms dominate in size due to the nature of the singularity in the electric potential. But, the interactions are produced by the off-diagonal terms and they get lost in the numerical calculations without some form of renormalization being applied to the matrix solver.

This study concerns just one critical aspect of IP data which is neglected in our experiences with inversion software. This aspect concerns the currents produced by the cover material when it the material is polarizable. In almost all instances, the cover material is polarized due to a variety of reasons such as weathering, moisture content, sediments and other material on the surface of the rocks hosting the anomalies.

Important Data Responses Not Reproduced in Inversion Software - Synthetic Study 1

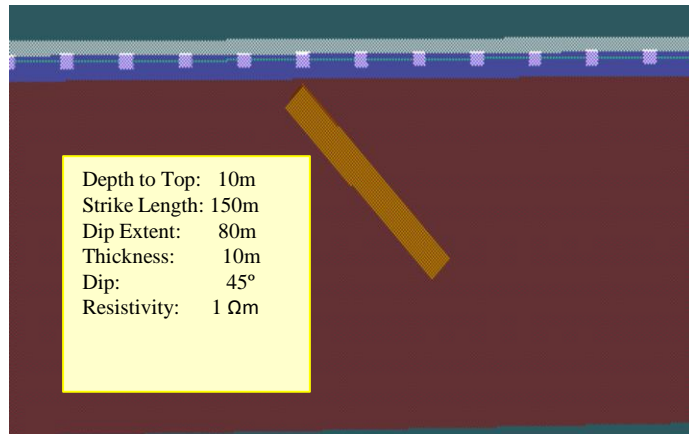


Survey Specifications and Models

The following modeling studies are based upon results from previous modeling work on IP data from surveys carried out in 2022/2023. The background resistivity structure is produced by a conglomerate over metamorphic rocks. The resistivity of the metamorphic rocks is taken as $600\Omega\text{m}$ as per both the dipole-dipole and gradient resistivity surveys. The conglomerate or cover is given a thickness of 8m from both forward and inverse modeling and this is consistent with drill results. The resistivity of the cover was set to $20\Omega\text{m}$ which was derived from the dipole-dipole data collected in summer whereas the gradient data collected in spring indicated the resistivity to be $10\Omega\text{m}$. This variation was determined to be due to the amount of moisture in the cover during spring as opposed to late summer. The polarizability of the cover is considered quite weak (0.5, 0.05, 1sec) for (C,m, τ) again derived from the dipole-dipole data but stronger during the gradient survey consistent with our moisture content hypothesis.

The variations in conductivity and polarizability of the cover dependent upon the season does not change the principal aspects of this study. This modeling study reuses the locations and survey parameters of a 50m dipole multi-line survey but we focus our results along one (L600) and for only for $N=1,4$. The four offsets and the one survey line are sufficient for the principal conclusions of the study. The following modeling studies are based upon results found our previous modeling work on the IP/resistivity data from the two surveys. The background resistivity structure consists of a conglomerate over metamorphic rocks. The resistivity of the metamorphic rocks is taken as $600\Omega\text{m}$ as per both the dipole-dipole and gradient IP/Resistivity surveys. The conglomerate or cover is given a thickness of 8m which was consistent with drill results and all our modeling of the data. The resistivity of the cover was set to $20\Omega\text{m}$ which was consistent with the dipole-dipole data collected in the summer although the gradient data collected in the previous spring indicated it was less than $10\Omega\text{m}$. The polarizability of the cover was found to be quite weak (0.5, 0.05, 1sec) for (C,m, τ) again consistent with the dipole-dipole data but stronger during the gradient survey consistent with our moisture content hypothesis. The variations in conductivity and polarizability of the cover dependent upon the season does not change the principal aspects of this study. The 3D model used in this study was determined from the actual survey data. After a number of trials, a thin dipping target was chosen. The target has a strike of 160m perpendicular to the line, a dip extent of 80m and a thickness of 10m and dipping at 45 degrees to the south with its bottom edge at a depth of 73m. The size, depth and dip of the target are taken from models produced to fit the resistivity data of the dipole-dipole and gradient surveys. The geometry of the target is not particularly important for the conclusions but as this study was related to interpretation of the actual surveys, we wished to use a model appropriate for the data to make the results more meaningful to our client. We utilize four permutations of the target, conductive ($1\Omega\text{m}$), resistive ($2000\Omega\text{m}$) and polarizable and non-polarizable. The polarizable parameters of the target (C,m, τ)=(0.5,0.8,5) are chosen quite large to more readily demonstrate the issues.

Important Data Responses Not Reproduced in Inversion Software - Synthetic Study 1



Survey Specs and Models, Cont'd

Electrode Array Parameters: This modeling study reuses the locations and survey parameters of a 50m dipole multi-line survey but we focus our results along one (L600) and for only for $N=1,4$. The four offsets and the one survey line are sufficient for the principal conclusions of the study. For several reasons, we have kept the Tx electrode size at 50m but reduced the Rx to 10m. Over a low resistivity cover which is also permeable, the depth of detection of the 50m dipole-dipole array is limited. A 50m Rx size tends to integrate and smooth the response and in the case of a conductor diminish the amplitude and variation of its response. Using the size of Rx to equal that of the Tx is traditional with the argument that this increases the measured voltage although it does reduce delineation. For, numerical purposes, we do not need a large Rx to enhance the voltage and accuracy of the response and thus we choose a Rx size of 10m for the increased delineation of the response.

Waveform and Windows: The current is a standard 8 second bi-polar signal. The original 20 time windows beginning with 280msec are utilized but additional early time windows are added to assist with understanding the responses (10,20,34,60,120, 200 msec). The window times are given with respect to their mid-times. The current turn off is a 1msec ramp in the simulations. The data in our surveys, of course, turned off much slower with an exponential turn off. The DC voltage or Resistivity calculation in the simulations is 250 msec prior to turn off well after the turn ON has maximized even with a slow turn ON exponential.

Plotting Reference Points: IP and resistivity data have traditionally been plotted and pseudo-sectioned with reference to the centre point (CP) of the array. The historical reason for this is unknown but probably relates to one dimensional resistivity sounding dating back almost 100 years. However, we have found and demonstrated that using the Tx and/or Rx location as a reference point can be very useful. Here, we utilize both the CP and Tx reference point approach. We also find it useful to deal with the on-time resistivity and off time IP data as in TDEM with common data units (i.e. mvolts). That is the resistivity data is simply an ON time window.

Synthetic Studies 1 – The field survey was from NNW to SSE but here we have rotated the survey to be N to S. The structures were roughly perpendicular to the survey lines and thus, here, the anomaly runs east to west and dips to the south. The survey can be thought to run from north (Stn 1100) to south (Stn 500) with the Rx leading the Tx from north to south.

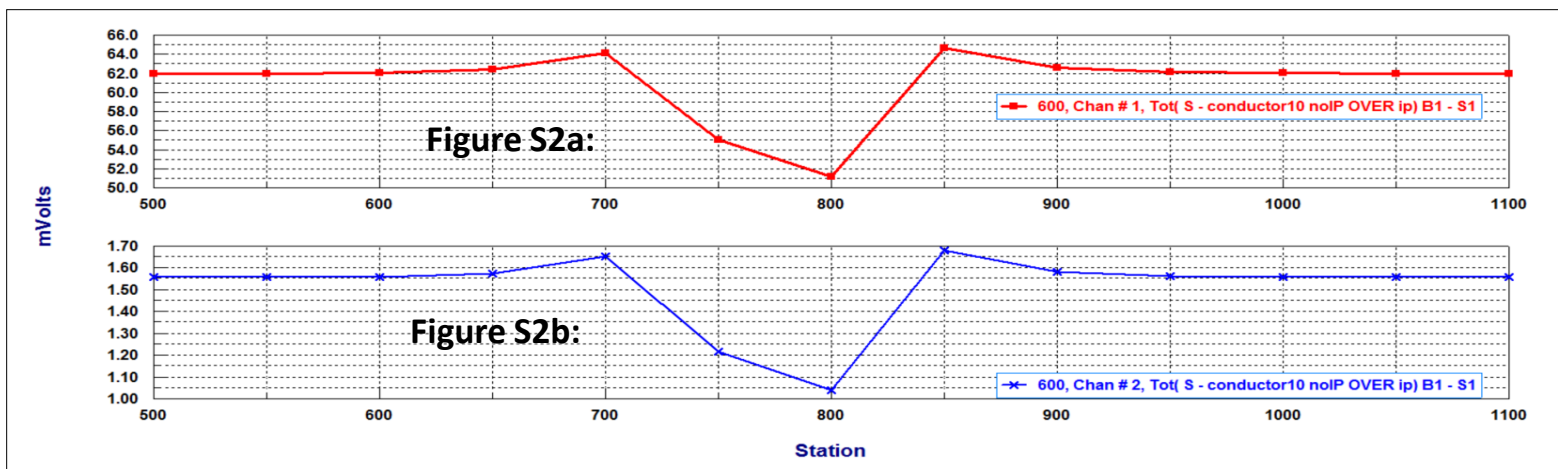
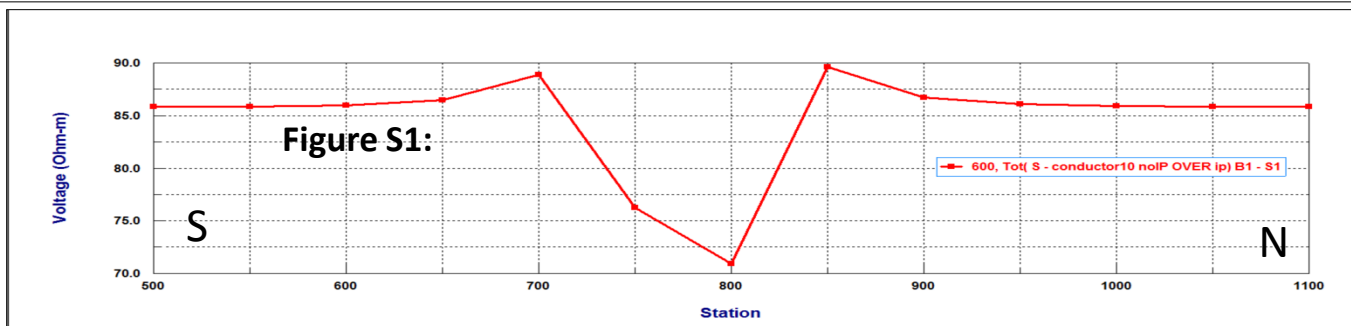
In Figure S1, the apparent resistivity is plotted of the on time window data for Model 1. We find it useful to sometimes interpret IP data in a similar manner to TDEM examining both ON and OFF time data in units of measurement. Thus, in Figure S2a, we display the ON time data in mvolts and in Figure S2b, the first OFF time window. We see, Figure S2b, that the current induced in the polarizable cover produces an off-time resistivity anomaly as the current continues to flow with the same geometry after turn off. This off time resistivity response will then decay as the currents in the cover.

Results I:

Model 1: Non-polarizable conductor under a polarizable cover.

Figure S1: The apparent resistivity for the 50m offset (N=1).

Figure S2: a) On time in mvolts and b) first off time (Ch2, 10msec) in mvolts



In Figure S3, decays are plotted including the on time for both the response of the cover plus basement (background) and the decay of the background plus the anomaly (total). The top figure is for the station (800) with the strongest resistivity response and the bottom figure for the station 50m to the east. The first 6 times windows are 10, 20, 35, 60, 120 and 200msec followed by the standard windows for an ELREC system with a time base of 2000msec per quarter period starting at 280msec.

Results II:

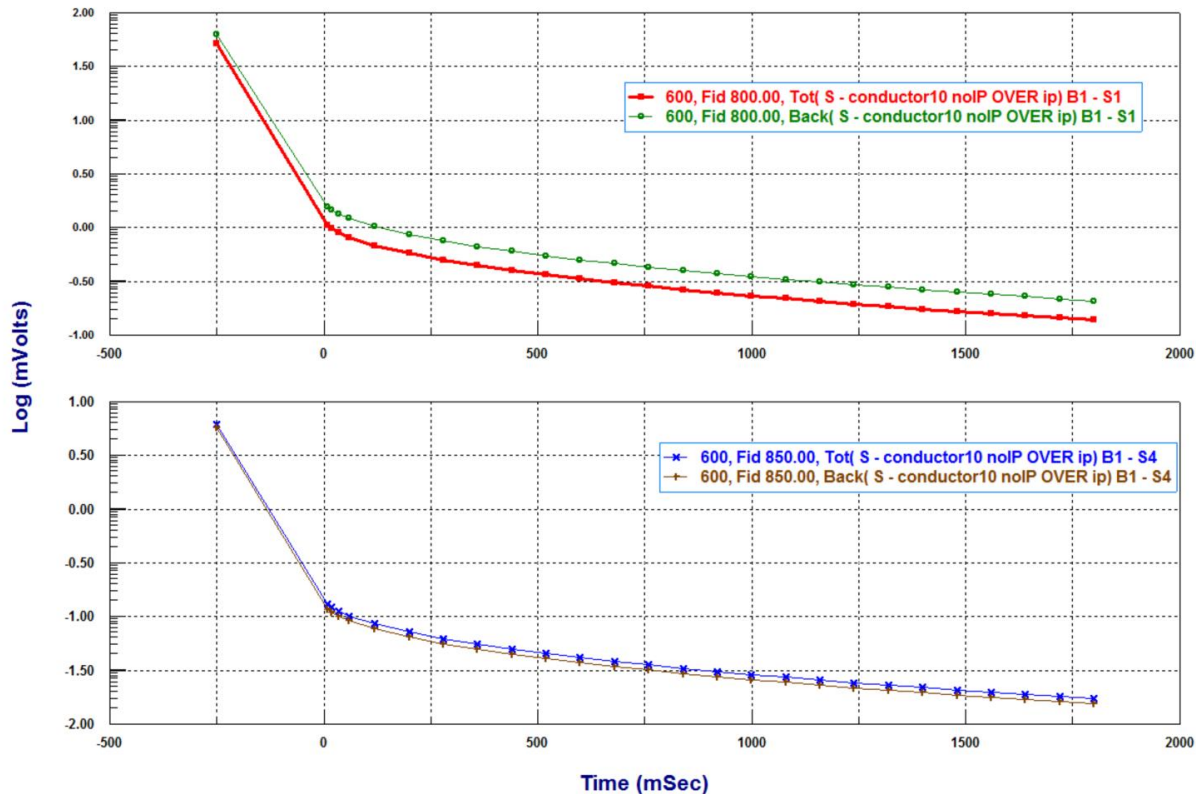
Model 1: Non-polarizable conductor under a polarizable cover.

Figure S3:

Top: Decay including ON time for the total (red) and the background (green) response at Stn800, 50m offset

Bottom: Decay including ON time for the total (blue) and the background brown) response at Stn850, 200m offset

Figure S3:



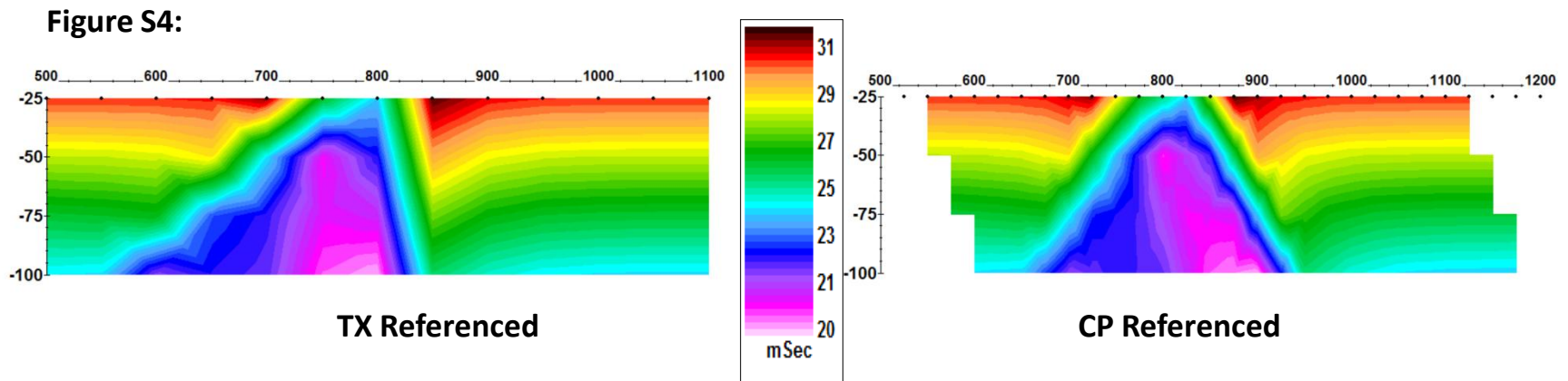
Model 1: Non-polarizable conductor under a polarizable cover.

Figure S4, displays the results as a pseudo-section with data transformed to the standard Newmont chargeability window and the depth is defined as half the separation length between the two closest electrodes of the TX and RX.

Results III:

Model 1: Non-polarizable conductor under a polarizable cover.

Figure S4: Standard Newmont Chargeability pseudo-section . [Left, Tx referenced] [Right, Centre Point referenced]



Discussion:

The currents produced in the cover by the polarizability of the surface materials continue into the off time. These off time currents naturally penetrate to depth and the conductor produces a secondary response in the off time when these currents interact with it. This behaviour is analogous to a current channeling response in the off-time in TEM data where the currents are induced during the turn off as opposed to being injected during on time in an IP response.

The source configuration drives currents into the resistive ground beneath the cover because the vertical current across the cover/basement boundary is essentially continuous.

These pseudo-sections could be interpreted as a polarizable target and we suggest that all commercial inversion software would produce a polarizable model.

Synthetic Studies

Results IV:

Model 2: Polarizable conductor under a non-polarizable cover. The same properties as Model 1 but now polarizable (pg2)

Figure S5: Apparent resistivity for the 50m offset (N=1).

Figure S6: N=2, On time in mvolts and first off time (10msec) in mvolts

Figure S5:

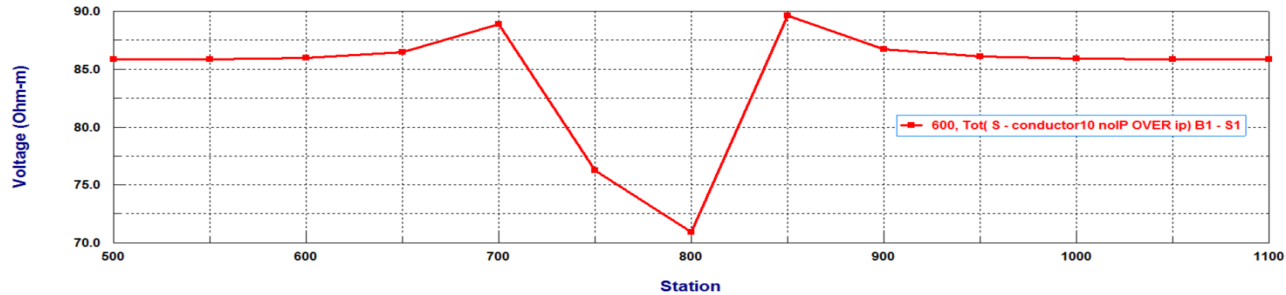
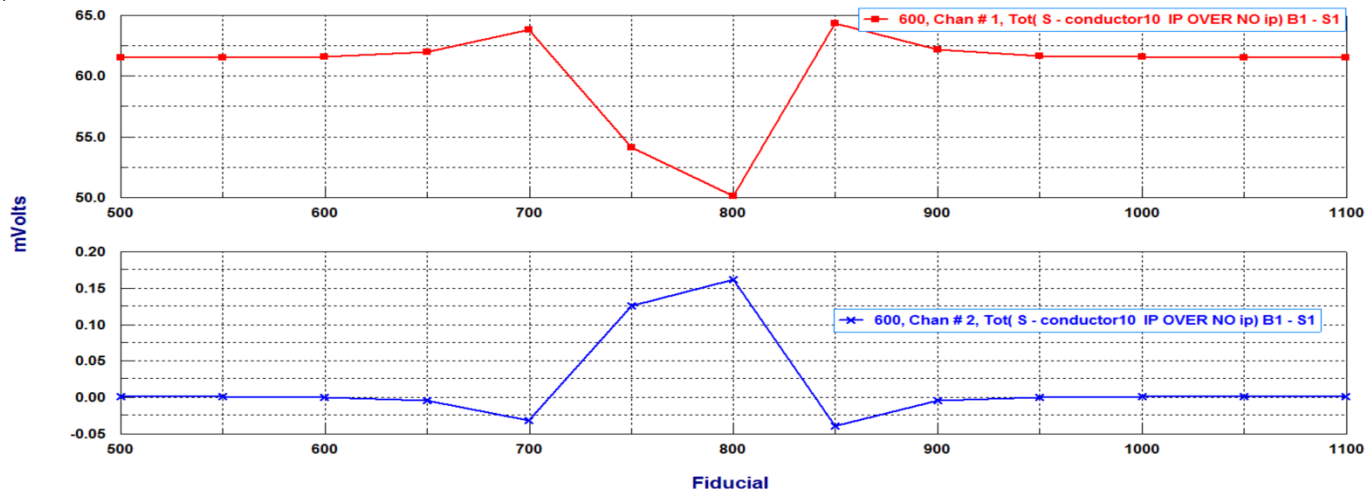


Figure S6:



Discussion:

The shape of the off time response is now a mirror image of the on time response. The secondary response has the opposite sign to the sign of the secondary response of the ON voltage. This is because the induced charges due to the polarizable anomaly oppose the exciting currents which are now the currents in response to the source of the background rocks..

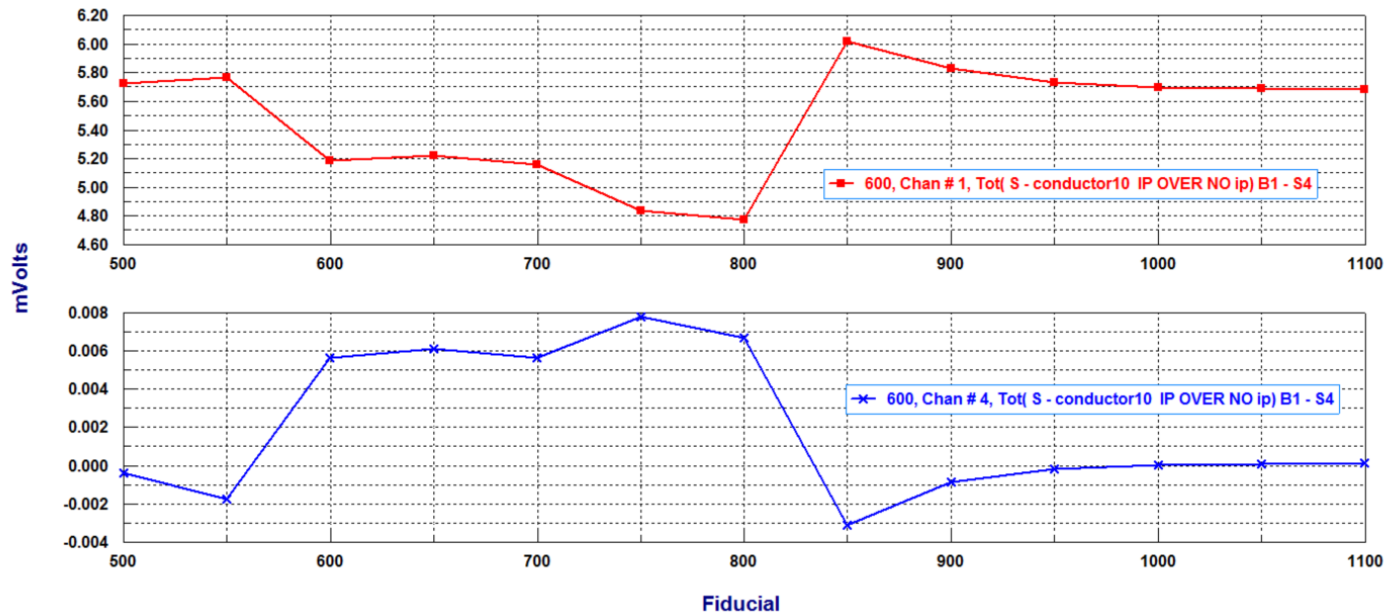
Synthetic Studies

Results V:

Model 2: Polarizable conductor under a non-polarizable cover.

Figure S7: On time voltage and third off time (34msec) for N=4.

Figure S7:



Discussion:

The exact mirror image as seen in N=1 at 10msec, continues for all separations and time windows excluding noise.

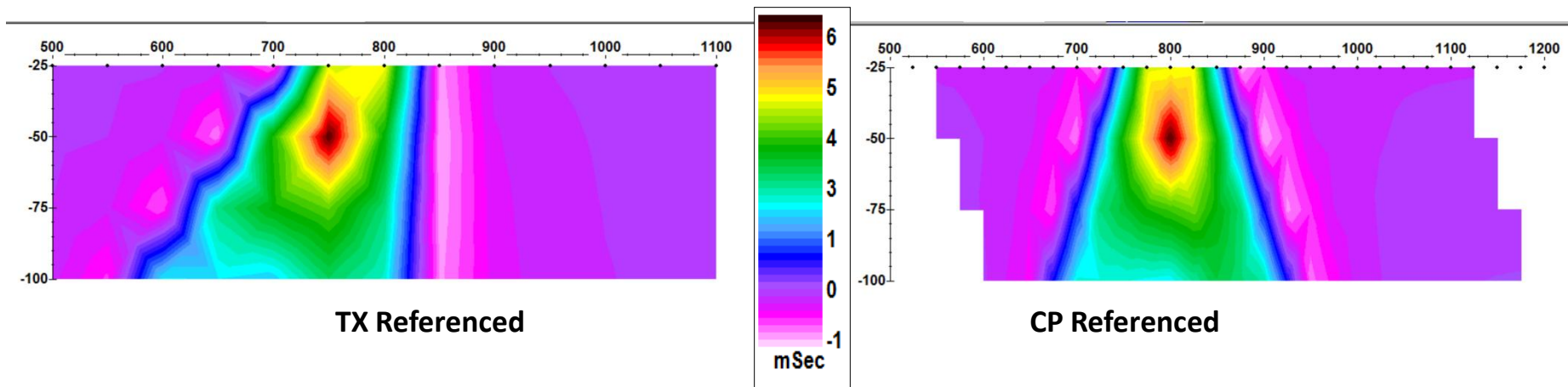
Synthetic Studies

Results V:

Model 2: Polarizable conductor under a non-polarizable cover.

Figure S8: Newmont Chargeability Pseudo-section

Figure S8: Model 2 Newmont Chargeability – Left – Tx referenced, Right – Centre Point (CP) referenced



Discussion:

The shape of the pseudo-section is now as expected with $N = 2$ (100m) having the largest response. The Tx referenced pseudo-section does indicate the southerly dip better than the CP representation.

Results VI:

Model 3: Polarizable conductor under a polarizable cover.

Figure S9 N=4, Apparent resistivity Model 1 vs Model 3.

Figure S10: N=3, 280msec window (instrument's Ch 1), Model 1 vs Model 3 (mvolts)

Figure S9
(small variation)

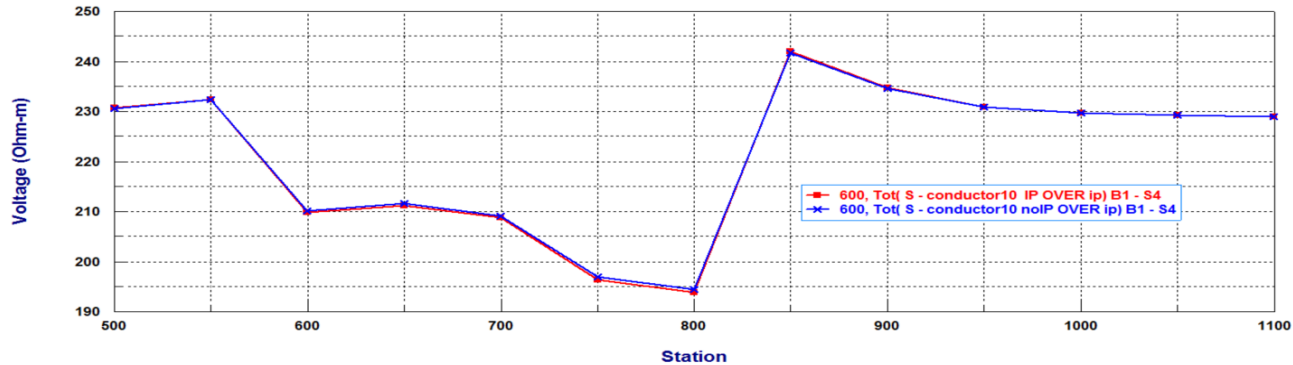
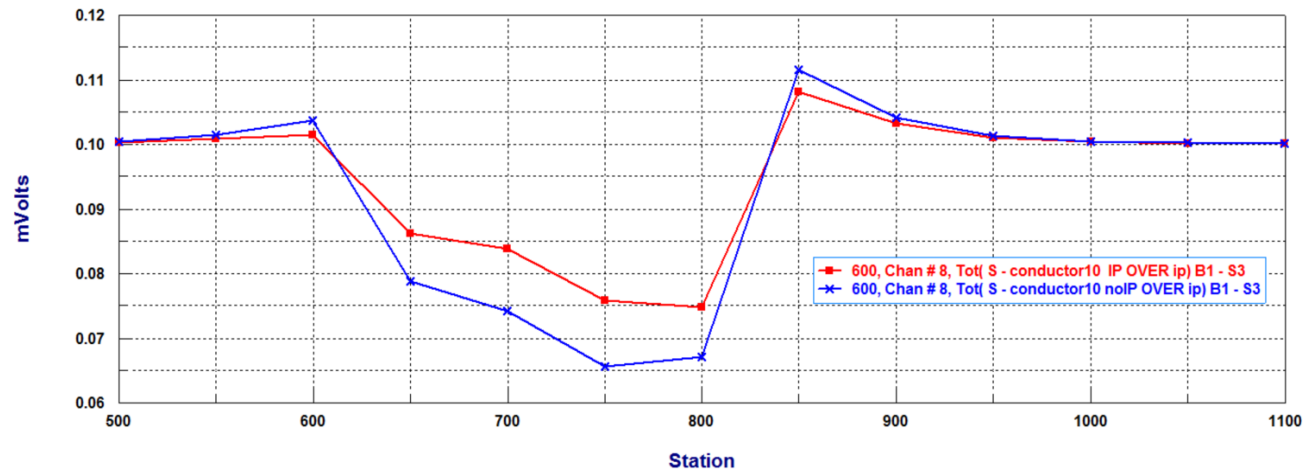


Figure S10:



Discussion:

As seen in Figure 6, the currents due to the polarization of the target are in opposition to the currents produced by the polarizable surficial currents. Thus, in this case, the polarizable conductor reduces the response of a non-polarizable conductor. *Note:* As the voltage channel is calculated as a wide window during the on time in analogy to most time domain IP instruments, there is a slight IP response in this window.

Results VI:

Model 3: Polarizable conductor under a polarizable cover.

Figure S11: Decays at Stn 750, **Model 1** vs **Model 3** in mvolts.

Figure S12: Same results as Fig11 but now normalized to primary voltage

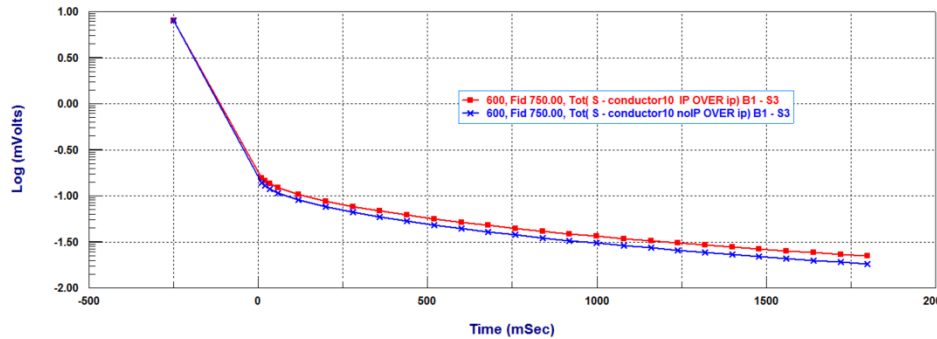


Figure S11

Model 1 decays as the response of the cover. The polarizable target essentially decays also as the cover layer (950 msec) for most of the off time. There is a small difference in the decay rate at very early time. The 3D anomaly has a much large τ than the cover but it is very difficult to distinguish this from the decay of the cover (Fig S11).

When normalized to the primary voltage as is customary, the slower decay of the target can start to be seen at later times. However, typical data quality in late time makes it almost impossible, in practice, to distinguish the polarizable conductor within the response of the polarizable cover.

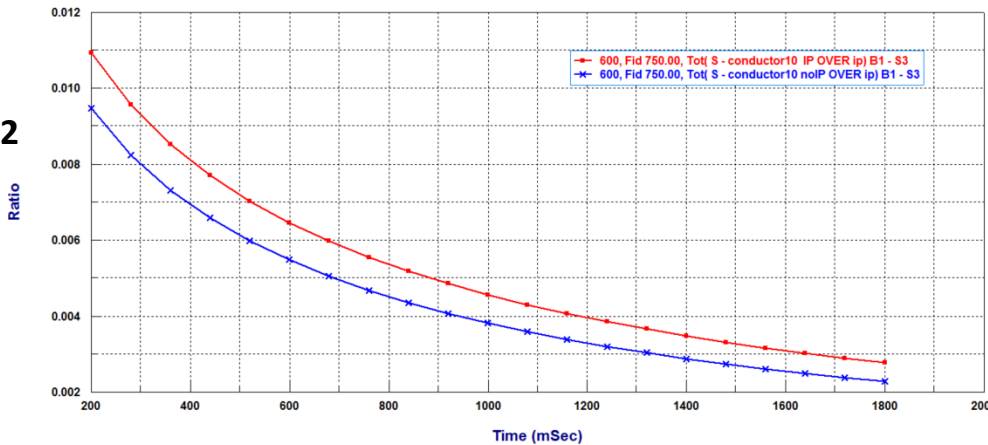


Figure S12

This result explained what was initially puzzling in our field survey. In particular, that the decays of the data were so consistent throughout all the data sites and in both the dipole-dipole and a gradient surveys. Secondly, the resistivity models for the surveys explained much of the off time data once a polarization was given to the covering conglomerate. This type of result, we have observed numerous times over the years with pole-dipole data but previously considered that the most likely source was polarizable material at the remote pole. Now, we would have to consider the possibility of the effects of the polarizable cover.

Synthetic Studies

Results VII:

Model 4: Non-polarizable resistor under a polarizable cover.

Fig S13: Apparent resistivity for the 150m offset (N=3).

Fig S14: On time in mvolts and 280msecs off time (Ch7) in mvolts

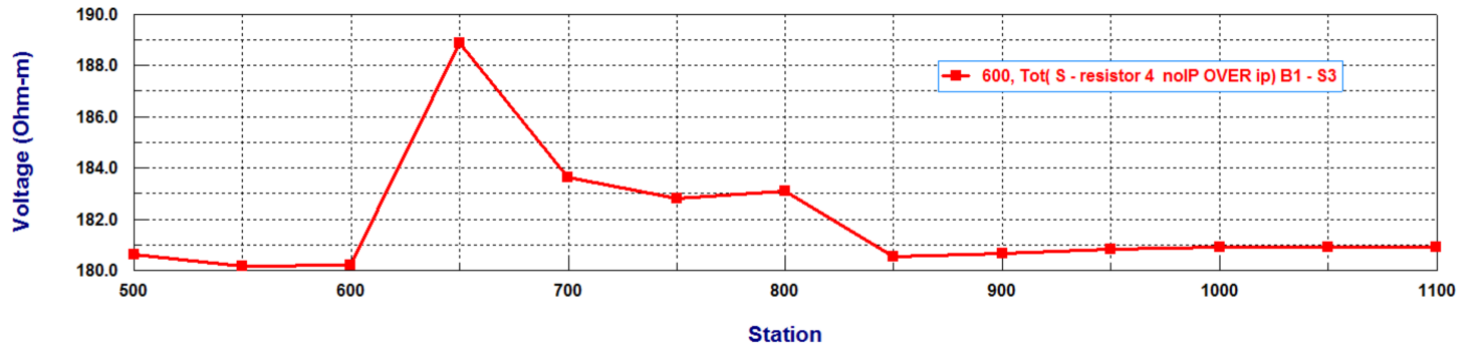


Figure S13:

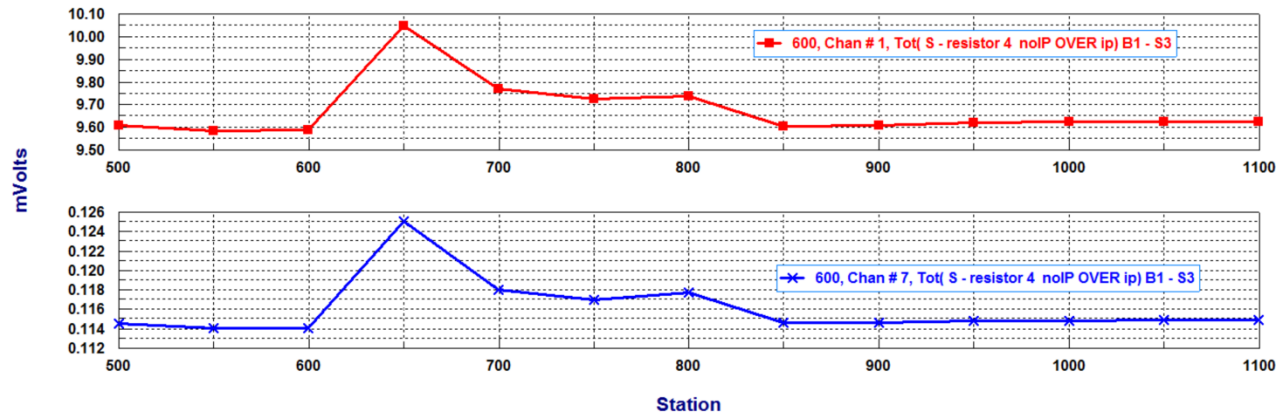


Figure S14:

Again, the off time response of the resistor has the same symmetry as the on time data and the decays at all stations are those of the polarizable cover.

Synthetic Studies

Results VIII:

Model 4: Non-polarizable resistor under a polarizable cover.

Figure S15a: Normalized Off time response, N=1, Total response compared to polarized cover (background) response

Figure S15b: Normalized Off time response, N=3

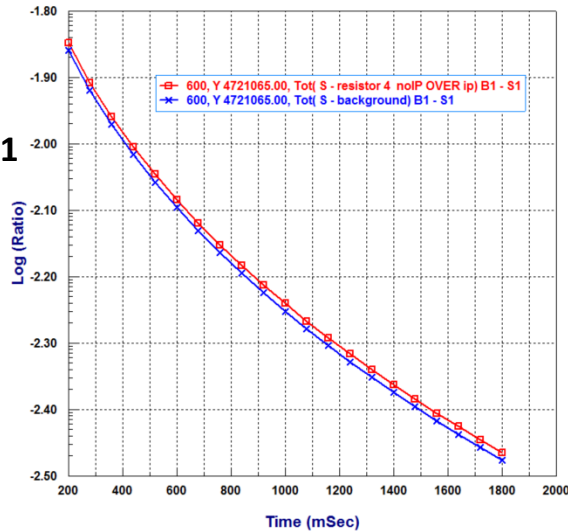


Figure S15a:
Stn 750, N=1

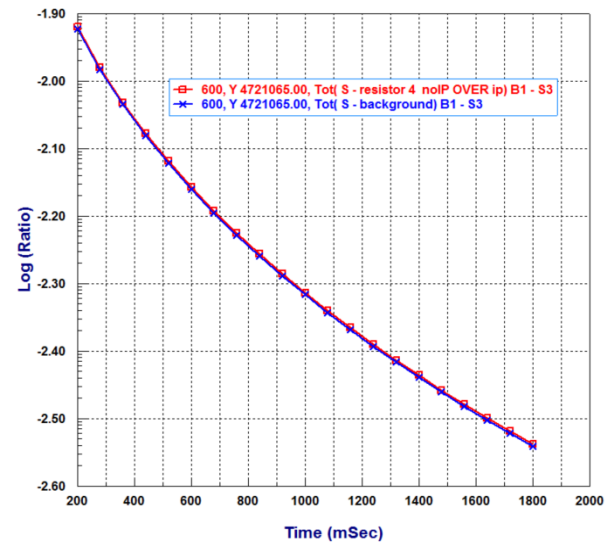


Figure S15b:
Stn 750, N=3

In the shortest offset, the response of the non-polarized resistor in the off time shifts the response of the background up a small amount. But, by N=3, there is almost no effect. One can consider the off time response of the anomaly as a static response due to the currents present in the earth during the off time created by polarizable cover. In the off time pseudo-section (Fig. S16), there is indication of an anomaly but probably not recognizable in typical survey noise. The resistor is, of course, seen clearly in the on time (resistivity) data (not shown here). Thus, no phantom IP target.

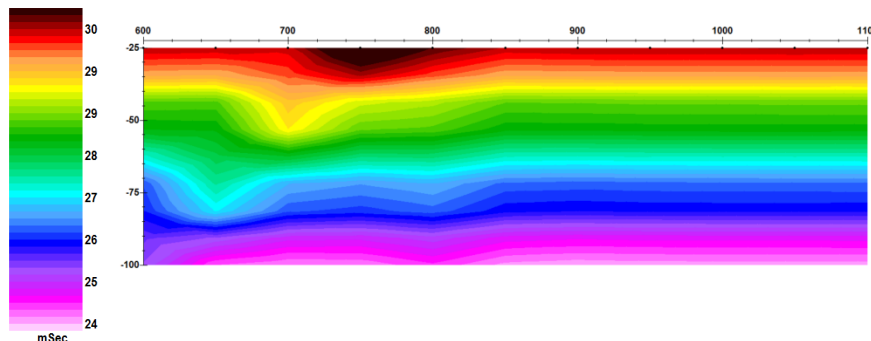


Figure S16:

Standard Newmont Chargeability:

Synthetic Studies

Results IX:

Model 5: Polarizable resistor under a non-polarizable cover. (Tx referenced)

Figure S17: Apparent resistivity for the 100m offset (N=2).

Figure S18: N=2, On time in mvolts and 280 msec (Ch7) in mvolts

Figure S17:

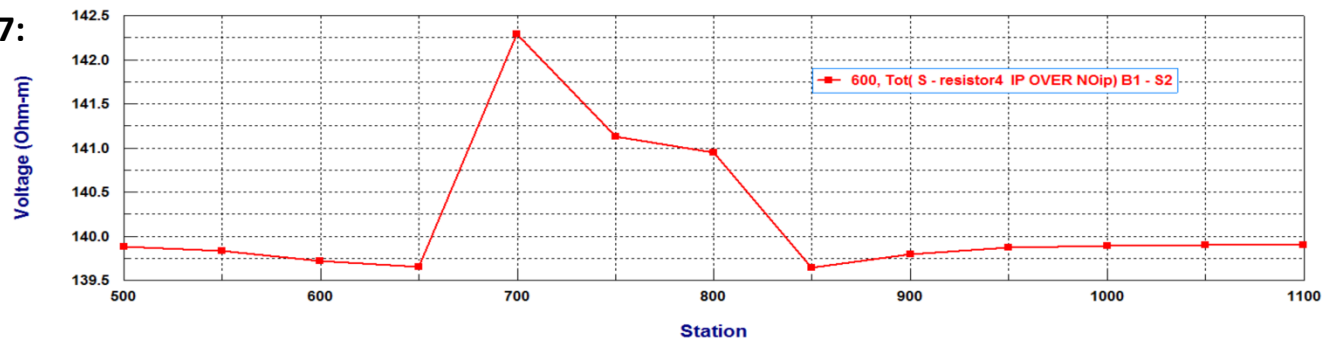
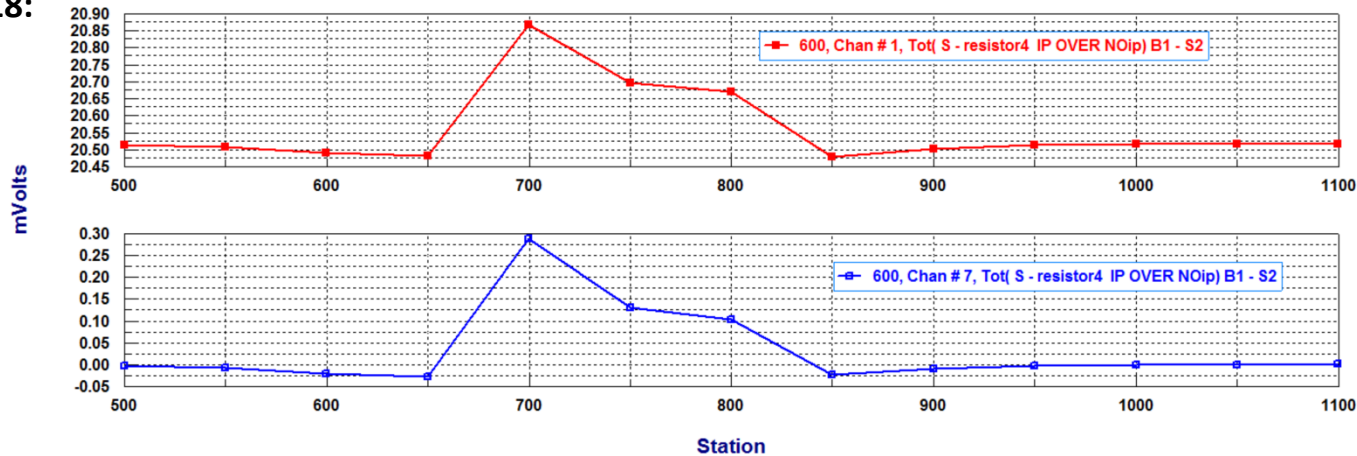


Figure S18:



Discussion:

Compared to results IV and V, the off time response of a polarizable resistor without a polarizing cover, is not the reverse mirror of the ON time voltage but the anomalous response in the OFF time has the same sign as the anomalous response in the ON time. The charges placed on the resistor during the on time simply decay due to the IP decay constant of the resistor. Thus, the response is the classical paradigm of an IP response.

Synthetic Studies

Results X:

Model 5: Polarizable resistor under a non-polarizable cover.

Figure S19: N=1, Total response (mvolts) compared to non-polarized cover (background) response

Figure S20: Newmont chargeability pseudo-section CP referenced (msec)

Figure S19: (Station 750)

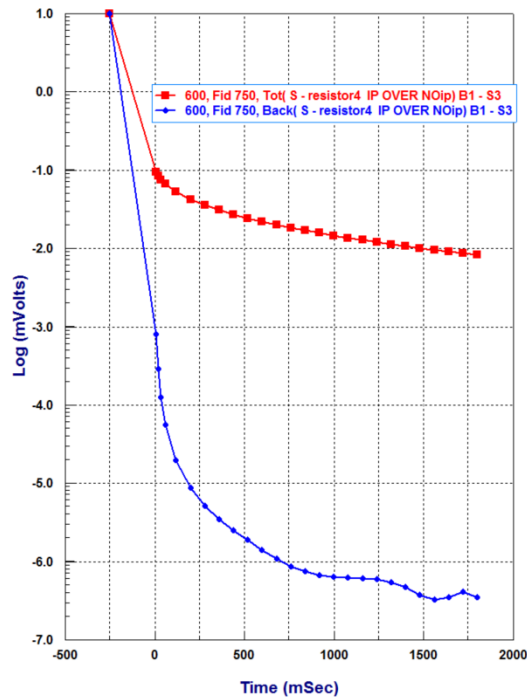
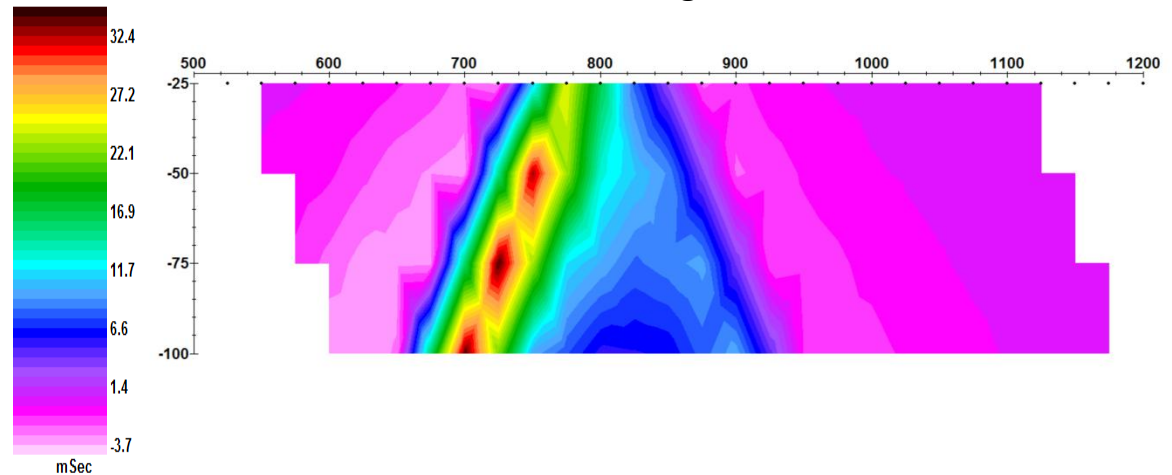


Figure S20:



Discussion:

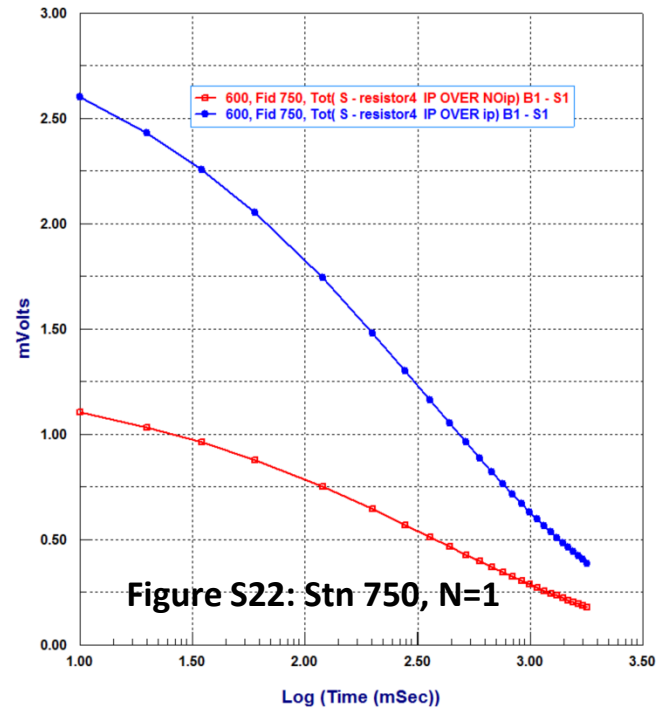
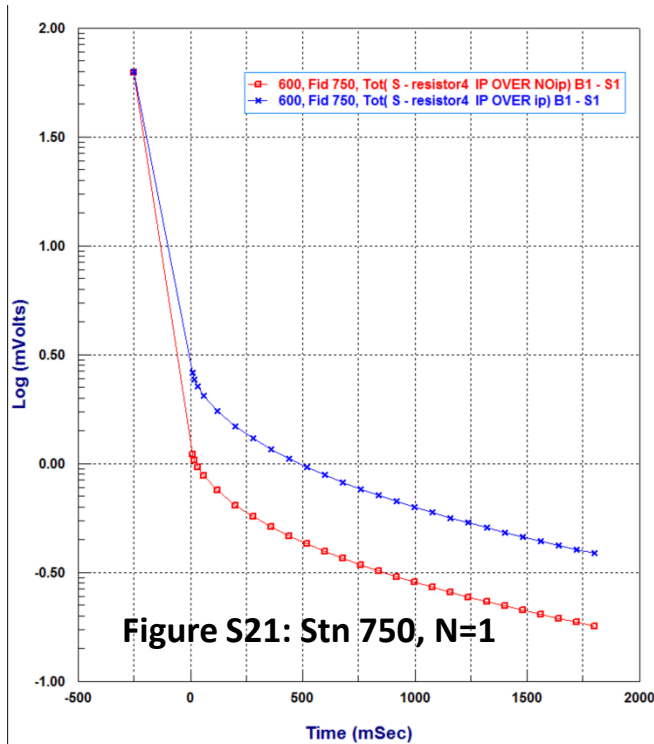
Figure S19 shows both the decay of the polarized resistor as well as the EM response (i.e. background response). Obviously, the EM response does not have to be considered in these models even at the earliest of time windows. The dip of the resistor is clearly obvious from the pseudo-section in CP reference. But, the halo of low apparent chargeability is enlarged by referencing the data to the centre point (see Figure 14).

Results X:

Model 5 vs Model 6: Polarizable resistor under a non-polarizable cover vs. Polarizable resistor beneath a polarizable cover

Figure S21: N=1, Comparison decays (red Model 5, blue Model 6). log voltage vs time

Figure S22: N=1, Comparison decays (red Model 5, blue Model 6). voltage vs log time



Discussion:

The effect of the polarizable cover is to increase the off time response and thus the “chargeability” in the off time. This is simply because the currents in the off time due to the polarizable cover induce additional charges on the resistor. Plotting the voltage response, for example, in Figure S21 appears to indicate that Model 6 is a constant additive shift above the response of Model 5. However, plotting voltage vs log time, we see that Model 6 is decaying faster in late time than Model 5. This is simply because the the decay constant for the cover is less than that of the resistor. However, the problem is more complicated as the polarizable cover induces currents which have a somewhat different geometry than the injected currents and the comparisons of Fig S21 and S22 are not exactly replicated at other stations. However, from a practical perspective, the main effect is the decreased drop immediately after turn off in Model 6 which will more or less be reproduced in any integrated “apparent chargeability” window as seen on the next page.

Synthetic Studies

Results XI:

Model 5 vs Model 6: Standard Pseudo-sections Newmont window. CP referenced.

Figure S23: Model 5, IP target over non-polarizable cover. Figure S24: Model 6, IP target over polarizable cover

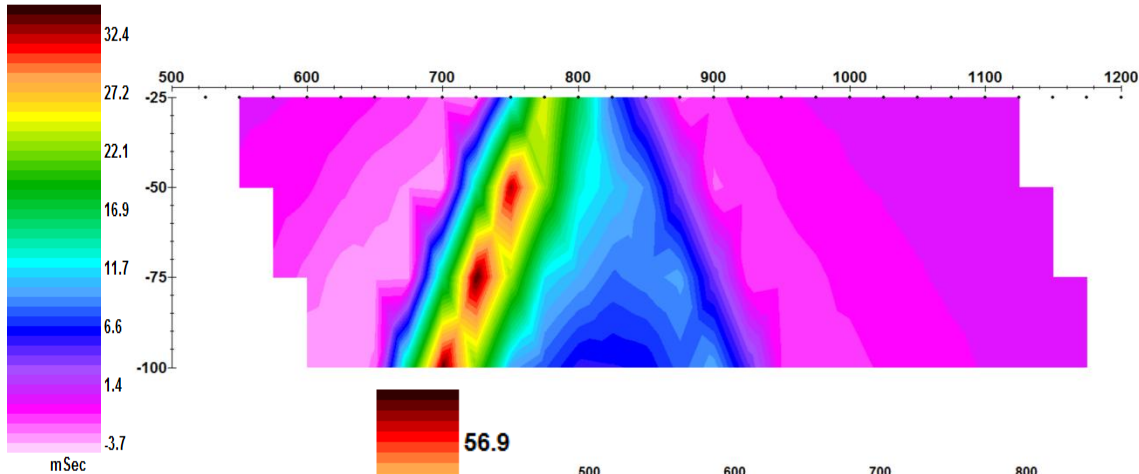


Figure S23:

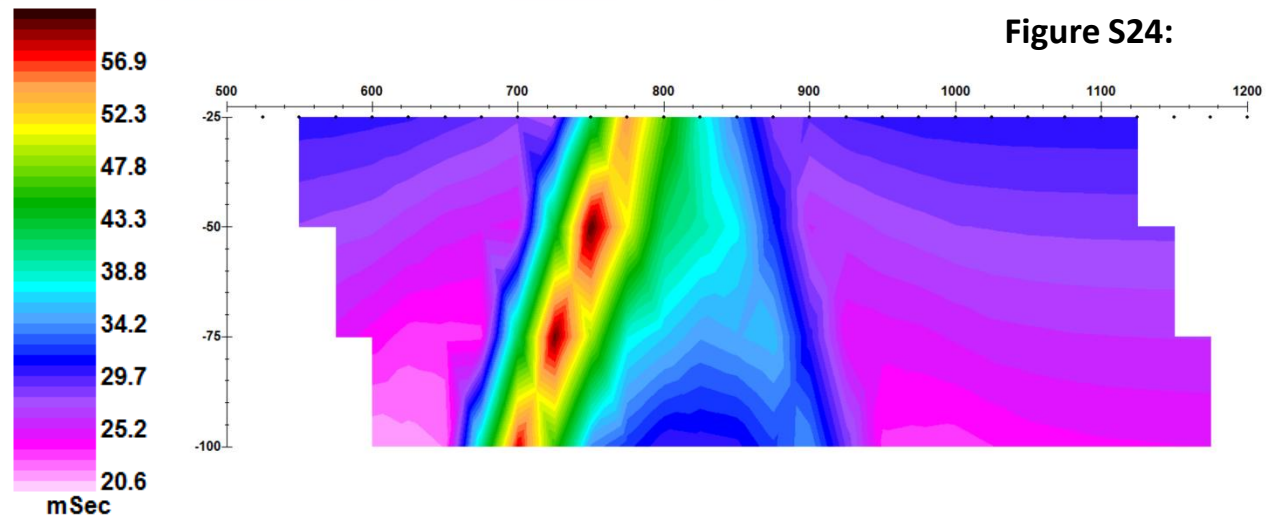


Figure S24:

Discussion: small “m”

Because of the sign of the secondary responses from the resistor due to being polarized, the polarizable cover increases the ratio of voltage immediately after turn off (V_p) to the voltage at the end of the on time (V_0) or the “m” chargeability. Without consideration in a model of the polarizable cover, the inference is that Figure 24 was due to target almost twice as polarizable as in Figure 23.

The capabilities of any inversion application are fundamentally limited by the accuracy and completeness of the forward algorithm utilized by the inversion app. One inversion may be faster or be able to find a lower residual but these are minor issues as compared to the forward algorithm. The establishment of an accurate 3D forward algorithm encompassing the major components of the physics involved is not a simple matter and this is especially true of EM processes including low frequency resistivity and IP studies.

The presence of a polarized cover is almost ubiquitous in IP surveys particularly in hard rock environments for mineral exploration. This is simply because the cover material is almost always highly weathered. Even if the weathering hasn't produced soil type materials, such as clay, it is still more porous and fragmented. Additionally, in hard rock environments there is often water contained at surface in one form or another as the rain and snow melt tend to stay on surface for some time due to the inability of the water to percolate to depth. Thus, this increases the conductivity of the cover over the substratum and thus a modified current flow into the substratum and these factors often produce a polarizable cover even if weakly polarizable. Even in sedimentary environments, depending upon the season and rainfall, the moisture content and increased weathering at surface can often produce a polarizable cover.

This modification of the electrical properties of the cover produces a difficult physical response for the typical finite difference and finite element inversion applications. The problems lie not in the inversion algorithms but rather in the associated forward algorithms. There are three (3) main physical responses that such codes have difficulty simulating.

1. Response of the Cover materials: This problem arises first in the basic resistivity response which must be simulated correctly in order to reproduce the current patterns in the subsurface interacting with the potential IP targets in the OFF time. As the cover is spatially large it requires the model to be extended out significantly beyond the survey area to obtain a reasonable simulated response to the model. Typically, in such forward algorithms (e.g. the UBC code), the solution does not converge. A typical requirement for any forward code is that as you increase the resolution of the grid cells, the solution converges on a particular response. Otherwise, one cannot determine when the simulated response is correct. Typically, when setting up a grid in an inversion application which is used also by the forward solution, the grid is not sufficiently fine or extensive over the cover material.

2. Generation of polarizable currents in the cover flowing into the subsurface: The common limitation of all 3D forward algorithms for electrical problems is the inability to produce current flow between one portion of the model and another. As mentioned, initially, this is not a problem of the mathematical formulation of the solution for the appropriate differential equation but a problem in the solving of the resultant matrix. This problem is caused by the nature of the fundamental singularity in the galvanic portion of the electric field potential. As regards, the currents produced by the cover, this is not an issue with IE techniques as the response of the cover layer is quasi-analytic and the resulting currents implant on the subsurface anomalies without any numerical difficulty (e.g University of Utah EM3D code). However, all commercial IP inversions utilize a finite difference or finite element approach.

3. Current interaction between anomalies: Similarly to the interaction of the polarizable cover with the deeper structures, there are interactions between the deeper structures as well as interactions within structures when the electrical properties have a gradients within the structure. As an example, are the models examined in this study with a polarizable cover. In such cases, there will be OFF time interactions between areas of different properties even if they are not polarizable. For the same reason that the effects of the induced polarization currents in the cover are not reproduced accurately in these 3D forward solutions and therefore their inverse applications, the interactions in the off time and ON time will not be recovered properly.

EMIGMA: While interpreting a survey using iterative forward models is not so simple as using a black box inversion, there are many benefits and with practice, the interpretation can be relatively fast. But, primarily when finished the user will now have a better understanding of the electrical property distribution and the responses to the injected currents.

The forward routines are very fast due to the numerical 3D techniques employed and the use of accurate quasi-analytic solutions to both the background response exciting the targets but also quasi-analytic techniques used to propagate the induced currents from the anomalies to the receivers.

One cost benefit is that generally one can obtain as accurate an interpretation from gradient surveys as dipole-dipole or pole-dipole survey thus substantially reducing the costs of data collection and also generally producing more accurate data for a range of reasons.